iScience

CellPress
OPEN ACCESS

Article

High-fat-diet-induced hepatic insulin resistance *per se* attenuates murine *de novo* lipogenesis

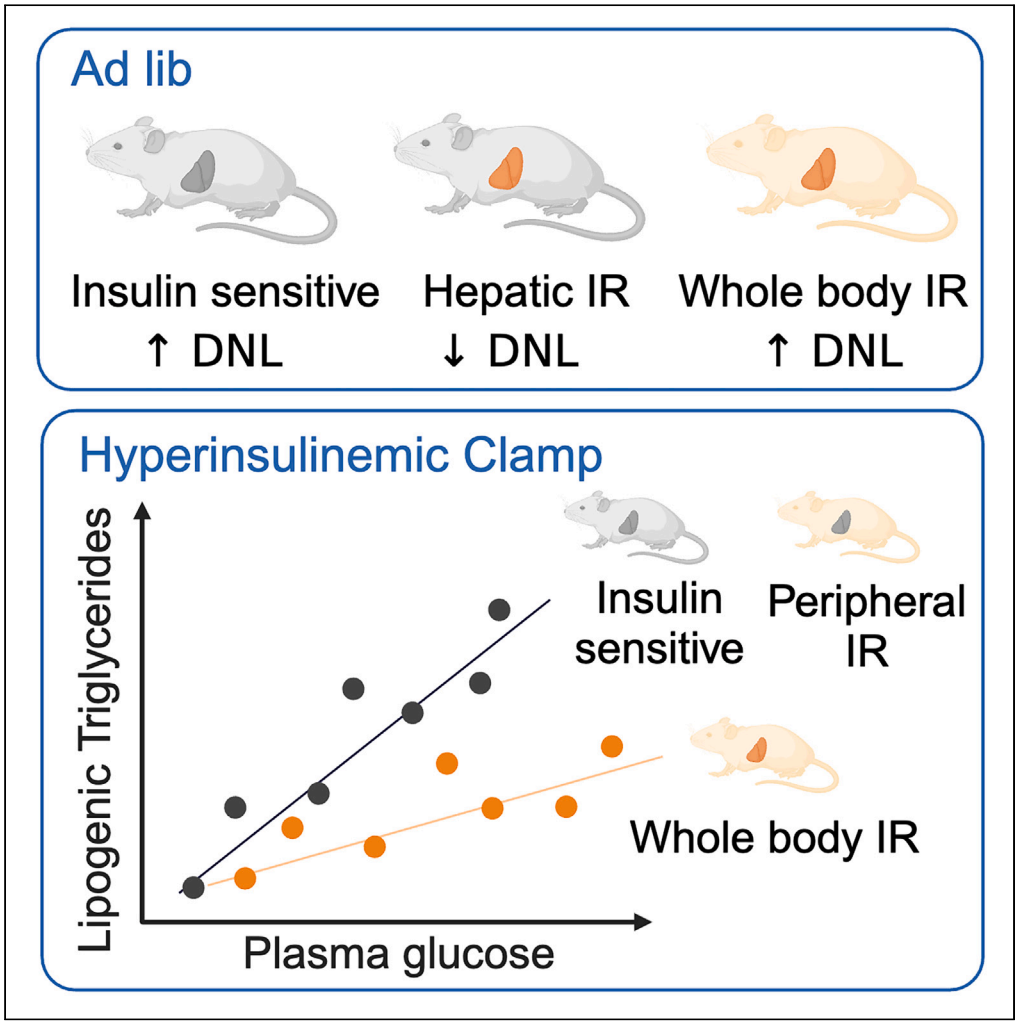

Leigh Goedeke, Jordan W. Strober, Rebecca Suh, ..., Varman T. Samuel, Gerald I. Shulman, Daniel F. Vatner

daniel.vatner@yale.edu

Highlights

Isolated hepatic insulin resistance (IR) reduces hepatic lipogenesis (DNL) in mice

Whole-body IR is associated with a rebound in hepatic DNL

DNL tracks with hyperglycemia in hyperinsulinemic mice and decreases with hepatic IR

Thus, hepatic insulin resistance is not pathway-selective in fat-fed mice

Goedeke et al., iScience 27, 111175
November 15, 2024
https://doi.org/10.1016/j.isci.2024.111175

iScience

CellPress
OPEN ACCESS

Article

High-fat-diet-induced hepatic insulin resistance *per se* attenuates murine *de novo* lipogenesis

Leigh Goedeke,[1,2,3,8] Jordan W. Strober,[1,8] Rebecca Suh,[1] Lauren M. Paolella,[1] Xiruo Li,[4] Jillian C. Rogers,[1] Max C. Petersen,[4,5] Ali R. Nasiri,[1] Gregori Casals,[1] Mario Kahn,[1] Gary W. Cline,[1] Varman T. Samuel,[1,6] Gerald I. Shulman,[1,4] and Daniel F. Vatner[1,6,7,9,*]

SUMMARY

Hepatic insulin resistance (IR) is often said to be "pathway-selective" with preserved insulin stimulation of *de novo* lipogenesis (DNL) despite attenuated insulin signaling toward glucose metabolism. However, DNL has not been assessed in models of liver-specific IR. We studied mice with differential tissue-specific lipid-induced IR achieved by different durations of high-fat diet (HFD) feeding. Mice with isolated hepatic IR demonstrated markedly reduced DNL, with a rebound seen in mice with whole-body IR. *Insr*^{T1150A} mice (protected against diacylglycerol-PKCε-induced hepatic IR) maintained normal DNL with HFD feeding. During hyperinsulinemic clamps, hepatic IR reduced DNL, but hyperglycemia augmented DNL in both resistant and sensitive animals. Regulation through SREBP1c did not consistently correlate with changes in DNL. These results demonstrate that hepatic IR is not pathway-selective, highlighting the primacy of lipogenic substrate in stimulation of DNL. Future therapeutics to reduce lipogenesis should target substrate drivers of DNL rather than targeting plasma insulin levels.

INTRODUCTION

Disordered lipid metabolism with high very low-density lipoprotein triglyceride (VLDL-TG) and low high-density lipoprotein (HDL) is a central feature of type 2 diabetes (T2D): atherosclerotic cardiovascular disease drives morbidity, mortality, and costs for patients with diabetes, and diabetes-associated nonalcoholic fatty liver disease (NAFLD) causes nonalcoholic steatohepatitis, cirrhosis, and hepatocellular carcinoma.[1,2] One well-described aspect of the dysregulated lipid metabolism of T2D is increased hepatic *de novo* lipogenesis (DNL) in the setting of insulin resistance and NAFLD,[3–7] and it has been suggested that DNL plays a role disproportionate to its contribution to hepatic lipid in the development of NAFLD.[4]

Insulin action drives DNL[8] through the master regulator SREBP1c,[9] whereas insulin's direct effect on the hepatocyte to suppress glycogenolysis, promote glycogen synthesis, and suppress gluconeogenic capacity is through activation of glycogen synthase and inhibition of FOXO1.[10] In insulin-resistant individuals, the observed increases in DNL are often attributed to insulin-mediated activation of SREBP1c, though these same individuals have defects in insulin-mediated activation of hepatic glycogen synthesis and suppression of hepatic gluconeogenesis. This disassociation between insulin-mediated regulation of hepatic lipid and glucose metabolism is described as paradoxical pathway-selective hepatic insulin resistance.[11] Molecular evidence for continued insulin-driven hepatic lipogenesis in insulin-resistant animals began with the demonstration that in the leptin-deficient *ob/ob* mouse, the expression of the insulin-driven master regulator of lipogenesis, *Srebp-1*, was increased as compared with wild-type (WT) mice.[12] Explanations for selective hepatic insulin resistance propose a signaling branchpoint dividing insulin action toward glucose metabolism and insulin stimulation of lipogenesis.[13–17]

If selective hepatic insulin action drives DNL in insulin-resistant patients, and DNL plays an important role in the pathophysiology of NAFLD[4] disproportionate to the insulin-independent process of esterification,[18] insulin as an early therapeutic option for T2D becomes a double-edged sword, normalizing glycemia at the expense of driving NAFLD. As yet, it is not clear whether insulin's impact on human hepatic lipid metabolism is detrimental. During hyperinsulinemic clamps, type 2 diabetic subjects demonstrated an increase in intrahepatic triglyceride content.[19] Furthermore, in a cross-sectional study of patients with T2D and NAFLD, insulin use was associated with an increase in biopsy-proven nonalcoholic steatohepatitis.[20] In contrast, in studies of 7–12 months duration, hepatic lipid content as assessed by magnetic

[1]Department of Internal Medicine, Yale School of Medicine, New Haven CT 06520, USA
[2]Cardiovascular Research Institute, Icahn School of Medicine at Mount Sinai, New York NY 10029, USA
[3]Diabetes Obesity & Metabolism Institute, Icahn School of Medicine at Mount Sinai, New York NY 10029, USA
[4]Department of Cellular & Molecular Physiology, Yale School of Medicine, New Haven CT 06520, USA
[5]Division of Endocrinology, Metabolism, and Lipid Research, Washington University School of Medicine, St. Louis MO 63110, USA
[6]Department of Medicine, Veterans Affairs Medical Center, West Haven CT 06516, USA
[7]Program in Translational Biomedicine, Yale School of Medicine, New Haven CT 06520, USA
[8]These authors contributed equally
[9]Lead contact
*Correspondence: daniel.vatner@yale.edu
https://doi.org/10.1016/j.isci.2024.111175

resonance spectroscopy (MRS) or magnetic resonance imaging (MRI), was observed to decrease with insulin therapy.[21,22] As insulin remains a mainstay of T2D therapy, a better understanding of the effects this treatment has on the underlying pathophysiology of T2D could influence treatment decisions and drive the discovery of future therapeutic targets.[23]

Pathway-selective models of hepatic insulin resistance imply that the signaling defect of insulin resistance occurs distal to such a branchpoint, an implication that is in conflict with the two best-studied models of lipid-induced cellular insulin resistance: ceramide-induced insulin resistance and diacylglycerol-induced insulin resistance.[24] Ceramide-induced insulin resistance attenuates insulin signaling by reducing the phosphorylation and translocation of Akt (protein kinase b),[25–27] whereas diacylglycerol-induced insulin resistance diminishes the tyrosine kinase activity of the insulin receptor itself.[28–30] In a weight-matched cohort of obese subjects with and without hepatic insulin resistance and NAFLD, we demonstrated an attenuation in insulin-mediated DNL in the insulin-resistant subjects.[7] Substrate-mediated DNL remained intact, and the carbohydrate-regulated insulin-independent transcription factor ChREBP (carbohydrate-responsive element-binding protein)[31,32] appeared likely responsible for changes in lipogenic capacity in these individuals. However, this study carried the usual limitations of human subjects research, lacking the detailed mechanistic power of the rodent studies that established the pathway-selective models of hepatic insulin resistance.

The observation of increased DNL in subjects with hepatic insulin resistance does not necessarily imply that insulin stimulation of DNL is preserved. An alternative hypothesis highlights the multiplicity of inputs into lipogenic signaling, both substrate and hormonal, and proposes that if these non-insulin drivers of DNL are active, it is unnecessary to invoke pathway-selective hepatic insulin resistance. The model of pathway-selective hepatic insulin resistance predicts that insulin continues to stimulate lipogenesis in insulin-resistant animals; however, this has not been clearly established *in vivo* in well-controlled models of insulin resistance. In the present work, we pursued a fundamental question: is insulin-driven lipogenesis increased in insulin-resistant mice? By establishing the existence (or lack thereof) of increased lipogenic insulin action, we hope to be able to provide focus for future studies of DNL in insulin-resistant and diabetic subjects.

RESULTS

Models of lipid-induced insulin resistance

To evaluate the effect of hepatic insulin resistance *per se* on the molecular regulation of lipogenesis and on rates of DNL, we took advantage of a useful feature of male rodent high-fat-diet (HFD)-induced insulin resistance. In these models, hyperinsulinemic clamp studies demonstrate that hepatic insulin resistance develops prior to whole-body/skeletal muscle insulin resistance,[28,33] allowing us to assess the impact of hepatic insulin resistance without the confounding effects of peripheral insulin resistance. Specifically, we used age-matched 9-day HFD-fed C57BL6/J mice to model hepatic insulin resistance in the absence of whole-body insulin resistance and 4-week (4w) HFD-fed C57BL6/J mice to model whole-body insulin resistance.

As dietary substrates themselves can impact DNL and confound comparison, modifications were made to the usual HFD models of insulin resistance to address two such confounders. First, differences in DNL between mice consuming two different diets could be related to differences in insulin action but could also be due to differences in dietary lipogenic substrate. Second, 60% HFDs contain very little substrate for DNL, with much less carbohydrate and protein than regular rodent chow, resulting in low signal-to-noise ratio in measurements of DNL. To minimize these confounders, we compared the 9-day and 4-week HFD fed mice to age-matched mice fed an HFD for 2 days. All mice also received drinking water containing 1% dextrose over the 2 days when ^2H_2O was used to quantify DNL. To validate that these modified HFD models still produce varying degrees of hepatic insulin resistance, we performed a modified insulin tolerance test (Figures 1A–1C, S1A, and S1B). Proximal insulin signaling, as measured by phosphorylation of Insr Y1162 and Akt S473, and insulin signaling down the lipogenesis and glycogen synthesis arms, as measured by phosphorylation of PRAS40 T246 and pGSK3β S9, decreased progressively between the 2-day, 9-day, and 4-week HFD models (Figures 1D–1G, S1C, and S1D). These changes mirror the changes in insulin action we have previously seen in hyperinsulinemic clamp studies in short-term and long-term HFD-fed mice.[28]

Lipogenic fluxes are attenuated by hepatic insulin resistance

Although DNL increases in insulin-resistant humans and mice,[4–7,34,35] lipogenic fluxes have not been assessed in animals with isolated hepatic insulin resistance and certainly not in isolated hepatic insulin-resistant animals fed identical diets. We next assessed lipogenic fluxes in *ad lib* fed mice using the deuterated water method (Figure 2A, left panel). In mice with predominantly hepatic insulin resistance (9-day),[28] DNL was decreased by more than half as compared with the less insulin-resistant group (2-day). As expected, all DNL measurements in fat-fed mice tended to be less than what we have observed in regular chow-fed mice under the same conditions (30% DNL ±4). With the development of comorbid skeletal muscle insulin resistance (4w),[28] rates of DNL rebounded nearly to baseline.

Calculation of lipogenic rates using the molar excess of deuterated palmitate may be confounded if hepatic triglyceride content is dramatically different between groups, as hepatic triglyceride synthesized prior to the introduction of deuterated water will be unlabeled, and differences in this pre-existing triglyceride will alter the calculated contributions of DNL. However, there was no significant difference in hepatic triglyceride content between the three groups (Table S1). If anything, the trend toward decreased triglyceride content in the 9-day group may have driven an underestimate of the magnitude in the decrease in lipogenesis in this group, but it would not have led to an overestimate of this decline.

Lipogenic fluxes in InsrT1150A mice are not significantly modified by HFD

HFDs suppress SREBP1c independent of alterations in insulin action.[36] The use of identical diets in our three groups should account for this potential confounder. However, to further segregate the role of hepatic insulin resistance from other effects of HFD feeding, we made use of

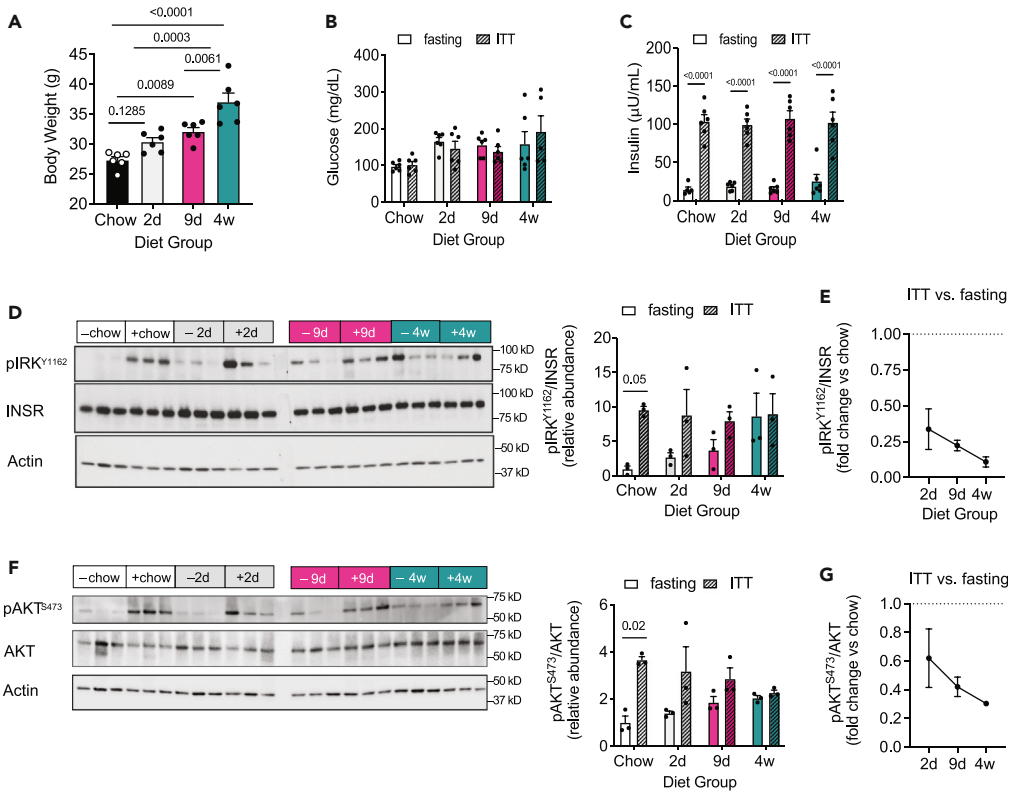

Figure 1. Proximal insulin signaling progressively decreases with duration of HFD feeding

(A–C) Body weight (A), plasma glucose concentrations (B), and plasma insulin concentrations (C) in male wild-type (WT) mice fed a chow diet or high-fat diet (HFD) for 2 days (2d), 9 days (9d), or 4 weeks (4w) and fasted overnight (fasting) or subjected to a modified intraperitoneal insulin tolerance test (ITT).

(D–G) Representative western blot analysis of pIRK^{Y1162}/INSR (D and E) and pAKT^{S473}/AKT (F and G) in the livers of mice treated as in (A–C). Quantification is shown to the right of each blot; actin was used as a loading control. Fold-change response to the ITT (versus fasting) is shown in (E) and (G), respectively. Fold-change response was normalized to chow-diet-fed animals (dotted line). n = 6 mice per treatment group. Data are represented as mean ± SEM. Statistical comparisons by one-way or two-way ANOVA with Tukey corrections for multiple comparisons or Kruskal-Wallis test with Dunn's correction for multiple comparisons where appropriate. All western blots are representative of samples (n = 3 per group) from the same experiment processed in parallel. Each dot represents a biological replicate.

See also Figure S1.

the *Insr*^{T1150A} mouse, a model protected against the development of diacylglycerol-PKCε-mediated insulin resistance.[28] *Insr*^{T1150A} mice were subject to the same three diet conditions that the WT mice were treated with. In this case, although DNL trended downward with 9-day HFD-feeding (consistent with some insulin-action-independent effects of HFD feeding), the DNL decreased to a lesser degree and the decrease was not significant (Figure 2A, right panel). Thus, lipid-induced hepatic insulin resistance *per se* reduces DNL in HFD-fed mice.

Hepatic glucose capture and storage

To assess whether differences in hepatic glucose uptake and storage could explain the differences seen in lipogenesis between the fat-fed animal models, we next measured hepatic glycogen content and hepatic glucose-6-phosphate content in fasted-refed WT and *Insr*^{T1150A} mice (Figures 2B and 2C). A trend was seen toward decreased refed glycogen content in the hepatically insulin-resistant 9-day HFD-fed WT mice (p = 0.06), and refed glucose-6-phosphate content increased with increasing duration of HFD in *Insr*^{T1150A} mice. However, these results do not clearly demonstrate whether substrate handling can explain the differences in lipogenesis observed.

Substrate drives DNL irrespective of insulin resistance in hyperinsulinemic-hyperglycemic clamps

DNL measurements under the dynamic conditions of fasting and feeding are impacted by multiple factors. In *ad lib* fed or fasting-refed mice, the lipogenic effects of increased circulating lipogenic substrate cannot be disentangled from the lipogenic effects of circulating insulin and other hormones. To evaluate the impact of lipogenic substrate availability on DNL, somatostatin-hyperinsulinemic-hyperglycemic clamps were performed (Figures 3A and 3B). The infused somatostatin suppresses secretion of several endogenous hormones, including insulin. 2-day fat-fed WT mice were used as a relatively insulin-sensitive control, 4-week fat-fed WT mice were used as model of whole-body insulin resistance, and 4-week fat-fed *Insr*^{T1150A} mice were used as a skeletal muscle insulin-resistant, hepatic insulin sensitive model.[28,33] Dextrose

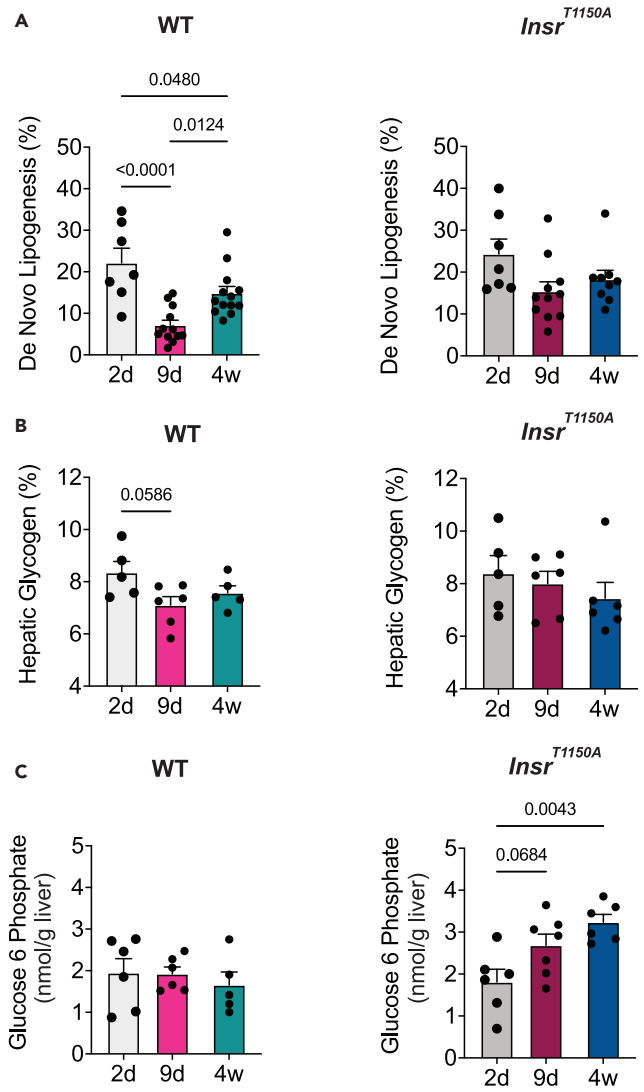

Figure 2. Hepatic insulin resistance *per se* suppresses DNL

(A) % DNL in the livers of wild-type (WT, left) or $Insr^{T1150A}$ mice (right) fed a high-fat diet (HFD) for 2 days (2d), 9 days (9d), or 4 weeks (4w). DNL was assessed by the deuterated water method. n = 7–13 mice per treatment group.

(B and C) Hepatic glycogen content (B) and hepatic glucose 6-phosphate concentration (C) in the livers of fasted-refed WT (left) or $Insr^{T1150A}$ mice (right) treated as in (A). n = 5–7 mice per treatment group. Data are represented as mean ± SEM. Statistical comparisons by one-way ANOVA with Tukey correction for multiple comparisons. Each dot represents a biological replicate.

See also Table S1.

was infused to target plasma glucose levels between 160 and 200 or 200–250 mg/dL. The average plasma glucose concentration achieved was proportional to net hepatic triglyceride synthesis during the clamp (Figure 3C). Notably, for the subset of mice clamped to modest hyperglycemia (<200 mg/dL), the 4-week HFD-fed WT mice with whole-body insulin resistance demonstrated significantly less accumulation of lipogenic hepatic triglyceride content than both groups of mice with preserved hepatic insulin sensitivity: the 2-day HFD-fed WT mice and the 4-week HFD-fed $Insr^{T1150A}$ mice (Figure 3D).

Hepatic glucose-6-phosphate, the first metabolite produced after glucose entry into the hepatocyte, and the direct substrates for lipogenesis (hepatic malonyl-CoA and acetyl-CoA), were assessed in hyperinsulinemic-hyperglycemic clamped liver tissue (Figures 3E, 3F, and S2A). Hepatic acetyl-CoA concentrations did not differ by group (Figure 3E). Hepatic glucose-6-phosphate was significantly decreased, whereas hepatic malonyl-CoA content was significantly increased, in the 4-week fat-fed $Insr^{T1150A}$ mice as compared with the 2-day and 4-week fat-fed WT mice (Figure 3F and S2A), suggesting that mice with genetic protection against hepatic insulin resistance shuttle more carbon into the precursor pool for DNL, possibly driven by elevated insulin levels and/or elevated insulin action (Figure 3B).

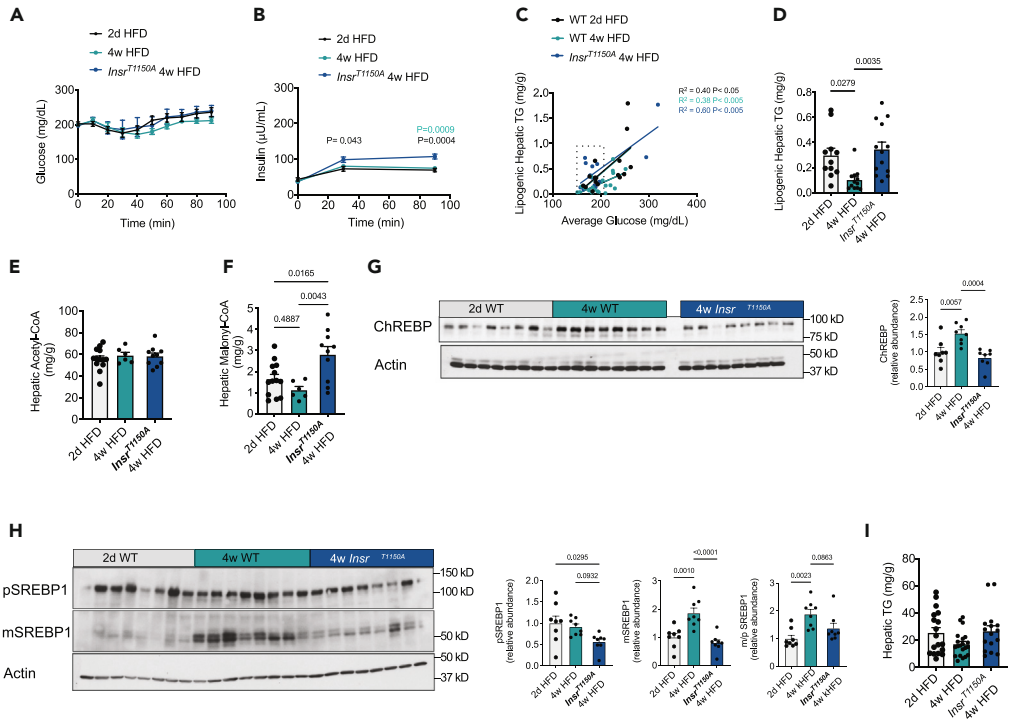

Figure 3. Substrate drives DNL irrespective of insulin resistance

(A–B) Plasma glucose (A) and insulin (B) achieved during a hyperinsulinemic-hyperglycemic clamp in 2-day (d) high-fat diet (HFD)-fed wild-type mice, 4-week (w) HFD-fed wild-type mice, and 4w HFD-fed *Insr*^{T1150A} mice. *n* = 15–21 mice per group.

(C) Lipogenic hepatic triglyceride content produced versus average glucose achieved during a hyperinsulinemic-euglycemic clamp. Data analyzed by linear curve fit (least squares fit). *n* = 11–13 mice per group.

(D) Lipogenic hepatic triglyceride synthesized in mice achieving an average glucose of ~150–200 mg/dL; see box outlined in (C). *n* = 11–13 mice per group.

(E and F) Hepatic acetyl-CoA content (E) and malonyl-CoA content (F) in mice treated as in (A and B). *n* = 6–13 mice per group.

(G and H) Hepatic ChREBP (G) and SREBP1 (mature and precursor) (H) protein expression in mice treated as in (A and B). Quantification is shown to the right of the blot. Actin was used as a loading control. *n* = 8 mice per group.

(I) Hepatic triglyceride content in mice treated as in (A and B). *n* = 16–21 mice per group. Data are represented as mean ± SEM. *n* = 8–20 mice per group. Statistical comparisons by one-way ANOVA with Tukey correction for multiple comparisons. All western blots are representative of samples from the same experiment processed in parallel. Each dot represents a biological replicate.

See also Figure S2.

Molecular regulation of *de novo* lipogenesis is attenuated by insulin resistance

Lipogenic protein abundance was assessed in livers from the intention-to-treat (ITT) experiment (Figures 4A–4F) and in fasted-refed mice (Figures S3A–S3C). ChREBP and SREBP1 (precursor form) protein abundance increased with increasing insulin resistance (Figures 4A–4C); however, no differences were seen in the ratio of mature to precursor SREBP1 forms (Figures 4A and 4C–4E). A trend toward increased *Srebf1* expression was observed between regular chow-fed mice and HFD-dextrose-water-fed mice, whereas *Chrebp1α/β* expression tended to decrease with HFD feeding (Figures S4A–S4C). Fatty acid synthase (FASN) was relatively matched in all groups, in both the ITT and fasting-refeeding experiments, both at the level of protein and mRNA (Figures 4A, 4F, S3A, and S4D). Total acetyl CoA carboxylase (ACC1 and ACC2) was also not significantly changed between fasting-refeeding groups (Figure S3B). Consistent with our ChREBP findings in the ITT study, L-pyruvate kinase (LPK), a factor responsive to ChREBP but not SREBP, was modestly increased in the 4-week fat-fed group as compared with the 2-day and 9-day groups (Figure S3C). Glucokinase gene expression was unchanged between groups (Figure S4E), and glucokinase protein abundance was modestly increased in the 9-day fat-fed group, the group that tended to have the lowest DNL contribution to triglyceride (Figures S2B and S2C). Thus, when dietary composition is controlled, progressive HFD-induced hepatic insulin resistance appears to minimally impair lipogenic protein abundance.

We next assessed hepatic ChREBP and SREBP1c content in the livers of hyperinsulinemic-hyperglycemic clamped mice (Figures 3G and 3H). Consistent with ChREBP expression in the ITT experiment, ChREBP expression was highest in the insulin-resistant group (4w HFD; Figure 3G). In contrast with the ITT experiment, SREBP1c processing was highest in the insulin-resistant group in the hyperinsulinemic-hyperglycemic clamp (4w HFD; Figure 3H). Interestingly, SREBP1c activation was higher in the insulin-resistant animals than the mutant animals (with higher clamped insulin levels, Figure 3B), suggesting that the increased SREBP1c activation sometimes seen in insulin-resistant liver may not be due to increased circulating insulin levels. Total hepatic triglyceride content was not different between the groups (Figure 3I).

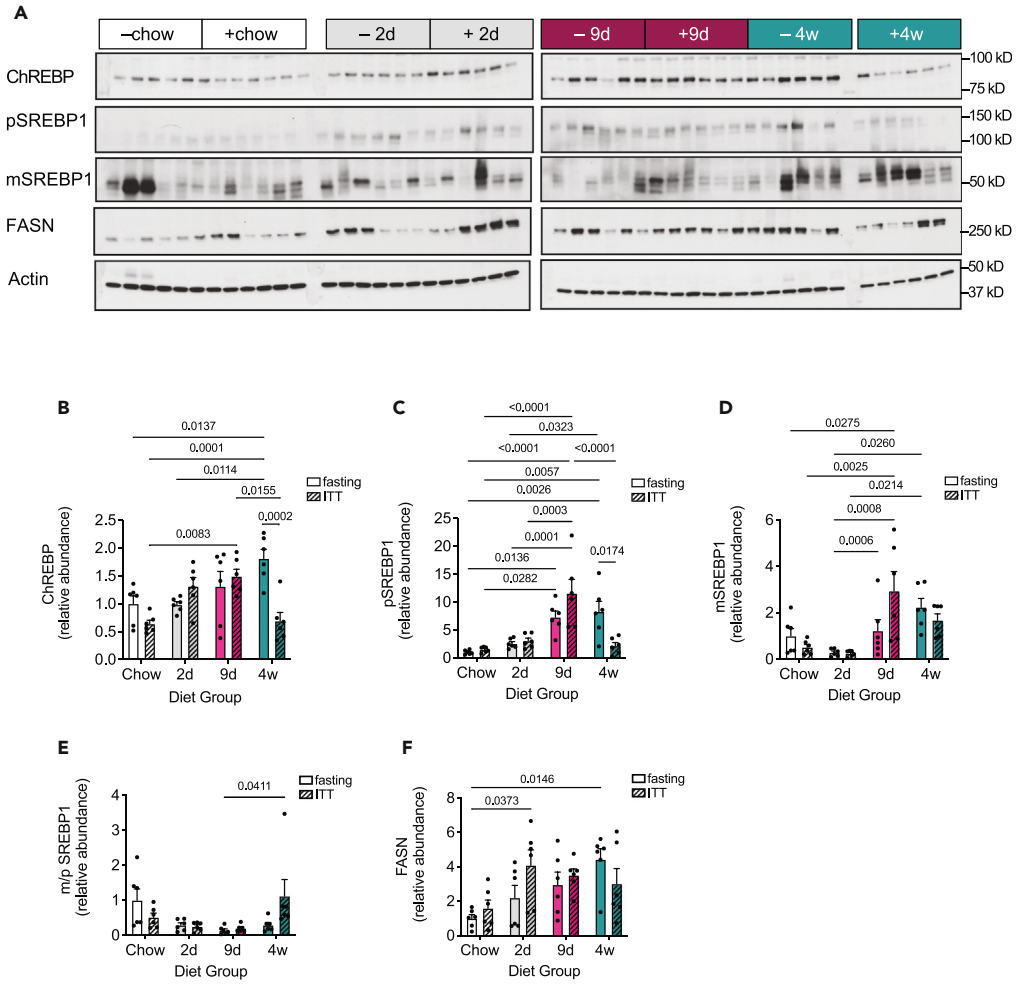

Figure 4. Molecular regulation of lipogenesis is attenuated by insulin resistance

(A) Western blot analysis of ChREBP, SREBP1 (precursor and mature), and FASN in the livers of 2-day high-fat diet (HFD)-fed (2d), 9-day HFD-fed (9d), and 4-week HFD-fed (4w) WT mice fasted overnight (–) or subjected to a modified ITT (+). Actin was used as a loading control. Quantification of blots shown in (B–F). $n = 6$ mice per group. Data are represented as mean ± SEM. Statistical comparisons by two-way ANOVA with Tukey correction for multiple comparisons. All western blots are representative of samples from the same experiment processed in parallel; internal controls were used for normalization of data when combining quantification from different blots. Each dot represents a biological replicate.

See also Table S1 and Figures S3 and S4.

Collectively, these hyperinsulinemic hyperglycemic clamps, combined with the data from the ITTs and *ad lib* fed lipogenesis experiments, demonstrate that although insulin is a critical regulator of hepatic lipogenesis, increased substrate availability (in this case, reflected by increased plasma glucose concentration) can promote hepatic lipogenesis in both insulin-sensitive and insulin-resistant models.

DISCUSSION

Hypertriglyceridemia and NAFLD are important pathologies associated with insulin resistance and T2D. While increased insulin-independent esterification of preformed fatty acids[18] may largely account for the increased triglyceride biosynthesis observed in insulin-resistant subjects, increased hepatic lipogenesis is thought to play an important role.[4,5] Pathway-selective hepatic insulin resistance was proposed to reconcile the important role of insulin in the regulation of lipogenesis with the increase in lipogenesis seen in insulin-resistant individuals[11] and continues to be widely invoked.[34,37] When we investigated hepatic lipogenic fluxes in obese humans, we observed increased DNL in insulin-resistant subjects after a meal, but no increase in DNL (and a decrease, if any change at all) in the setting of glucose-stimulated hyperinsulinemia, and no pathway selectivity of insulin signaling.[7] In this human study, we could not isolate hepatic insulin resistance from confounders that impact hepatic lipogenesis. Many of the mechanisms by which insulin signaling can drive mTOR (mammalian target of rapamycin) and SREBP1c have been elucidated *in vitro* and *in vivo* in genetically insulin-resistant and insulin-sensitive rodents,[12,13,38] but these models cannot address the question of whether hepatic insulin resistance is a pathway-selective process.

In the present experiments, we were able to isolate lipid-induced hepatic insulin resistance from other lipogenic drivers. The paradigm of pathway-selective hepatic insulin resistance predicts that given similar fat and carbohydrate intake, animals with increasing levels of hepatic insulin resistance should have increased SREBP1c-driven DNL due to circulating hyperinsulinemia. Contrary to this prediction, during *ad lib* feeding we found that lipid-induced hepatic insulin resistance potently attenuates hepatic lipogenesis, and this inhibition is mitigated after the development of skeletal muscle insulin resistance and the associated increased availability of circulating lipogenic substrate (e.g., glucose in the present studies). In hyperinsulinemic-hyperglycemic clamp studies, HFD-fed mice with hepatic insulin resistance demonstrated the lowest rates of lipogenesis when hyperglycemia was limited, but DNL increased with increasing circulating substrate regardless of the extent of insulin sensitivity/resistance. Finally, measures of molecular regulators of lipogenesis did not correlate well with differences in lipogenic contribution to triglyceride synthesis: (1) no differences were seen in lipogenic protein abundance (particularly FASN) between insulin-sensitive and insulin-resistant groups, and (2) SREBP1c activation (cleavage) varied between experiments and did not correlate with lipogenic rates. It was certainly a surprise that none of the molecular regulators of lipogenesis were either clearly increased or decreased in the animals with altered lipogenic rates, but these findings underscore our conclusion that although molecular regulation of DNL is known to be important, one cannot look to molecular regulation as a readout of lipogenesis physiology. The paradoxical pathway-selective model of hepatic insulin resistance cannot be reconciled with these findings.

In addition to demonstrating that hepatic insulin resistance is not pathway-selective, these experiments also underscore the important permissive role of insulin action in the regulation of DNL. Loss of lipogenic drive has been seen previously in studies of the liver insulin receptor knockout mouse (LIRKO[39]), in our own studies of rats treated with antisense oligonucleotide (ASO) targeting the insulin receptor[18] and in Akt knockout mice.[40] Furthermore, mice with defects in the canonical insulin signaling pathway demonstrate significant defects in hepatic triglyceride synthesis.[41,42] However, insulin resistance is not the same thing as absence of insulin action, which is underscored when comparing the relative hepatic insulin resistance of short-term HFD-fed mice[28,33] with the profound loss of both the anabolic and mitogenic effects of insulin on the liver in the LIRKO mouse.[43] As such, we did not see as dramatic a decrease in hepatic lipogenesis in our insulin-resistant animals as was seen in LIRKO and insulin receptor ASO-treated animals, and we did not observe a decrease in lipogenic enzyme content by immunoblotting. In addition to the effect of reduced but present insulin signaling on lipogenic protein abundance, the increase in ChREBP and L-PK observed in whole-body insulin-resistant refed mice suggests that the lipogenic transcription factor ChREBP[31,32] may play a role as well. Substrate flux into hepatic lipogenic pathways (from both carbohydrate and protein sources) can also drive increased lipogenesis: skeletal muscle deletion of *Slc2a4* (the insulin-regulated glucose transporter GLUT4) leads to accelerated hepatic lipogenesis in mice,[44] whereas humans with skeletal muscle insulin resistance have increased rates of carbohydrate-stimulated DNL.[6] Furthermore, endoplasmic reticulum (ER) stress can drive SREBP1c activation without input from insulin signaling.[45,46] Making the interpretation of the literature on this topic more complex, none of the mechanisms driving lipogenesis is completely autonomous of all other mechanisms; for example, in the absence of hepatocellular insulin action, ChREBP activation decreases,[39] as would be expected when insulin-stimulated glucokinase[47,48] decreases. Furthermore, insulin may impact hepatocyte Srebp1c action independent from traditional hepatocyte insulin signaling, for example, when IRS-1 or IRS-2 are knocked out, *Srebp1c* is unaffected.[17] Nevertheless, in the present studies, (i) restoration of near-normal levels of lipogenesis in whole-body insulin-resistant mice, along with (ii) the steady increase in lipogenesis seen with increased substrate flux during the hyperinsulinemic-hyperglycemic clamps regardless of degree of hepatic insulin resistance, taken together suggest that altered substrate flux can account for DNL in the insulin-resistant animal.

One of the strengths of this study is the use of animal models that allow us to isolate hepatic insulin resistance from insulin resistance in other tissue beds. Although such extreme tissue specificity is not typically seen in prediabetic patients, this tissue specificity allows us to address the question of the role of hepatic insulin action separate from insulin action in other tissues and may begin to provide insight into how precision medicine approaches may be applied based on heterogeneity in tissue-specific insulin resistance between patients. Another strength of this study is the use of the $Insr^{T1150A}$ model as a hepatically sensitive model. This model has been rigorously evaluated by hyperinsulinemic-euglycemic and hyperinsulinemic-hyperglycemic clamps for tissue-specific insulin action.[28] Furthermore, this model is specifically designed to test diacylglycerol-nPKC-induced insulin resistance, a form of insulin resistance that is clearly relevant to human patients. In obese humans, hepatic diacylglycerol content[49–51] and hepatic PKCε translocation[50,51] are associated with insulin resistance, and indeed, insulin receptor T1160 phosphorylation (homologous to the rodent insulin receptor T1150) is associated with insulin resistance in obese patients as well.[29]

Notably, in this discussion, we have been using glucose flux as a surrogate for the changes in substrate flux seen in the insulin-resistant mouse. However, carbohydrates may not be the primary source of carbon for lipogenesis in mice.[52] The question of which fluxes play an important role in DNL in the insulin-resistant organism is a fascinating, open question, the pursuit of which could open new understanding of the dysfunctional lipid metabolism associated with insulin resistance.

Additionally, only one HFD was used in this study, one which contains saturated fat-rich lard and polyunsaturated fat-rich soybean oil in approximately a 10:1 ratio. Using multiple diets with different fatty acid composition can have a large impact on the results of a study like this one—high PUFA diets suppress SREBP activation,[36] whereas high saturated fat diets can drive inflammation (a phenomenon called "meta-flammation").[53,54] The use of identical diets during the measurement of lipogenesis, and the use of multiple mouse models to isolate hepatic insulin resistance from other factors, are strengths of the design of these studies, allowing us to essentially rule out the existence of pathway-selective hepatic insulin resistance. Thus, the increased DNL seen in most insulin-resistant individuals would be expected to be due to a combination of factors: altered substrate fluxes are likely driving lipogenesis, whereas lipogenic capacity is maintained in part by residual insulin action and in part by the carbohydrate-regulated transcription factor ChREBP. Individual hepatic substrate fluxes may drive particular

processes—one may drive DNL leading to NAFLD, whereas another may drive lipotoxic metabolite synthesis, leading to hepatic insulin resistance. Future studies are warranted to dissect the roles of individual substrate fluxes on DNL and determine how alterations in lipogenic capacity does (or does not) impact rates of lipogenesis.

In sum, combining these findings in HFD-fed mice with the prior observations in obese human subjects,[7] we see that hepatic insulin resistance respects the orthodoxy of proximal lipid-induced insulin resistance. Rather than selectivity between pathways, hepatic insulin resistance affects glucose and lipid metabolism in a pathway-promiscuous manner. Other actors, such as lipogenic substrate flux, are required for the increased DNL seen in insulin-resistant subjects. As such, the clinician using insulin in insulin-resistant patients is doing more to protect the liver from excess lipogenic substrate flux and fatty acid flux than they are causing dysregulated lipogenesis (consistent with studies of insulin treatment in diabetes patients[21,22]). Furthermore, investigational therapeutic strategies that divert substrate from the liver, divert carbons from anabolic to catabolic pathways, or prevent calories from being consumed will be the most effective for prevention of hepatic triglyceride biosynthesis in the progression to NAFLD.

Limitations of the study

Several limitations of this study merit mentioning. First, during the hyperinsulinemic-hyperglycemic clamp, the 4-week HFD-fed *Insr*^{T1150A} mice achieved a 25%–33% higher plasma insulin concentration than the two groups of WT mice, likely due to altered insulin clearance in the mutant mice. Thus, we cannot quantitatively determine the degree to which differences in lipogenic triglyceride observed between these mice and WT mice should be attributed to improved hepatic insulin action versus increased circulating insulin. However, when reviewing the differences in lipogenic triglyceride content from the clamp studies that achieved modest hyperglycemia (160–200 mg/dL), it would be reasonable to suspect the difference in insulin may account for the trend toward ~20% increase in DNL seen as compared with the 2-day HFD-fed WT group and far less likely to account for the 4-fold difference in DNL as compared with the 4-week HFD-fed WT group. Second, the *Insr*^{T1150A} knockin is a whole-body knockin. As such, we cannot rule out changes in inflammatory cell insulin action, or central nervous system insulin action, altering rates of lipogenesis in the mutant mice. Furthermore, while the *Insr*^{T1150A} knockin demonstrates diacylglycerol-induced skeletal muscle insulin resistance, and thus appears to be peripherally insulin resistant on hyperinsulinemic clamp,[28] other tissues may be protected to some degree (e.g., white adipose tissue[55]) contributing to the observed phenotype of the *Insr*^{T1150A} knockin mouse. Third, as noted earlier, HFDs suppress SREBP1c independent of alterations in insulin action.[36] We paid careful attention to this issue, using dextrose in drinking water to increase lipogenic substrate availability and using the *Insr*^{T1150A} knockin to separate the effects of lipid on insulin action from the direct effects of lipid on lipogenesis. Nevertheless, lipogenic rates in these mice were less than what is seen in high-carbohydrate (regular chow)-fed mice. Although low lipogenic rates mimic human physiology,[5,7,56,57] such low rates also impose a limitation on the dynamic range of our measurements. Finally, the use of male mice alone also deserves mention, as ideally one would study models of both sexes. However, the tissue-specific insulin resistance with HFD-feeding required for this study is a characteristic of male mice,[58] and so females were excluded.

RESOURCE AVAILABILITY

Lead contact

Further information and requests for resources and reagents should be directed to and will be fulfilled by the lead contact, Daniel Vatner (daniel.vatner@yale.edu).

Materials availability

This study did not generate new unique reagents.

Data and code availability

- All data reported in this paper will be shared by the lead contact upon request.
- This paper does not report original code.
- Any additional information required to reanalyze the data reported in this paper is available from the lead contact upon request.

ACKNOWLEDGMENTS

We would like to thank Gina Butrico, John Stack, Wanling Zhu, Xiaoxian Ma, Codruta Todeasa, and Maria Batsu, and the Yale Diabetes Research Core facilities (Yale School of Medicine) for excellent technical support. Graphical abstract was created with BioRender.com.

This study was supported by grants from the United States Public Health Service, National Institutes of Health (R00 HL150234 (L.G.), R01 DK124272 (D.F.V.), R01 DK116774 (G.I.S.), R01 DK119968 (G.I.S.), K23 DK102874 (D.F.V.), T32 DK007058, the Yale Diabetes Research Center P30 DK045735); and the Veterans Health Administration (I01 BX000901 [V.T.S.]).

AUTHOR CONTRIBUTIONS

Conceptualization, L.G., V.T.S., G.I.S., and D.F.V.; methodology, L.G., M.C.P., A.R.N., G.W.C., and D.F.V.; formal analysis, G.W.C. and D.F.V.; investigation, L.G., R.S., J.W.S., L.M.P., X.L., J.C.R., A.R.N., G.C., M.K., D.F.V.; resources, G.I.S. and D.F.V.; writing—original draft, L.G. and D.F.V.; writing—review & editing, L.G., J.W.S., M.C.P., G.W.C., V.T.S., G.I.S., and D.F.V.; visualization, L.G. and D.F.V.; supervision L.G., G.W.C., V.T.S., G.I.S., and D.F.V.; funding acquisition, L.G., V.T.S., G.I.S., and D.F.V. All authors reviewed the manuscript critically for intellectual content, and all authors approved the final version.

DECLARATION OF INTERESTS

The authors declare no competing interests.

STAR★METHODS

Detailed methods are provided in the online version of this paper and include the following:

- KEY RESOURCES TABLE
- EXPERIMENTAL MODEL
  - Animal care
- METHOD DETAILS
  - *In vivo* hepatic *de novo* lipogenesis
  - Fasting-refeeding studies
  - Tissue triglyceride extraction
  - Measurement of triglyceride *de novo* lipogenesis
  - Immunoblotting
  - Quantitative PCR
  - Hyperinsulinemic-hyperglycemic clamp studies
  - Modified insulin tolerance tests
  - Plasma biochemical assays
  - Short chain CoA, glycogen, and glucose-6-phosphate measurements
- QUANTIFICATION AND STATISTICAL ANALYSIS
  - Statistics

SUPPLEMENTAL INFORMATION

Supplemental information can be found online at https://doi.org/10.1016/j.isci.2024.111175.

Received: June 28, 2023
Revised: January 4, 2024
Accepted: October 10, 2024
Published: October 15, 2024

REFERENCES

1. American Diabetes Association (2018). Economic Costs of Diabetes in the U.S. in 2017. Diabetes Care *41*, 917–928. https://doi.org/10.2337/dci18-0007.
2. El-Serag, H.B., Tran, T., and Everhart, J.E. (2004). Diabetes increases the risk of chronic liver disease and hepatocellular carcinoma. Gastroenterology *126*, 460–468. https://doi.org/10.1053/j.gastro.2003.10.065.
3. Hellerstein, M.K., Schwarz, J.M., and Neese, R.A. (1996). Regulation of hepatic de novo lipogenesis in humans. Annu. Rev. Nutr. *16*, 523–557. https://doi.org/10.1146/annurev.nu.16.070196.002515.
4. Donnelly, K.L., Smith, C.I., Schwarzenberg, S.J., Jessurun, J., Boldt, M.D., and Parks, E.J. (2005). Sources of fatty acids stored in liver and secreted via lipoproteins in patients with nonalcoholic fatty liver disease. J. Clin. Invest. *115*, 1343–1351. https://doi.org/10.1172/JCI23621.
5. Lambert, J.E., Ramos-Roman, M.A., Browning, J.D., and Parks, E.J. (2014). Increased de novo lipogenesis is a distinct characteristic of individuals with nonalcoholic fatty liver disease. Gastroenterology *146*, 726–735. https://doi.org/10.1053/j.gastro.2013.11.049.
6. Petersen, K.F., Dufour, S., Savage, D.B., Bilz, S., Solomon, G., Yonemitsu, S., Cline, G.W., Befroy, D., Zemany, L., Kahn, B.B., et al. (2007). The role of skeletal muscle insulin resistance in the pathogenesis of the metabolic syndrome. Proc. Natl. Acad. Sci. USA *104*, 12587–12594. https://doi.org/10.1073/pnas.0705408104.
7. Ter Horst, K.W., Vatner, D.F., Zhang, D., Cline, G.W., Ackermans, M.T., Nederveen, A.J., Verheij, J., Demirkiran, A., van Wagensveld, B.A., Dallinga-Thie, G.M., et al. (2021). Hepatic Insulin Resistance Is Not Pathway Selective in Humans With Nonalcoholic Fatty Liver Disease. Diabetes Care *44*, 489–498. https://doi.org/10.2337/dc20-1644.
8. Topping, D.L., and Mayes, P.A. (1982). Insulin and non-esterified fatty acids. Acute regulators of lipogenesis in perfused rat liver. Biochem. J. *204*, 433–439.
9. Brown, M.S., and Goldstein, J.L. (1997). The SREBP pathway: regulation of cholesterol metabolism by proteolysis of a membrane-bound transcription factor. Cell *89*, 331–340.
10. Petersen, M.C., Vatner, D.F., and Shulman, G.I. (2017). Regulation of hepatic glucose metabolism in health and disease. Nat. Rev. Endocrinol. *13*, 572–587. https://doi.org/10.1038/nrendo.2017.80.
11. Brown, M.S., and Goldstein, J.L. (2008). Selective versus total insulin resistance: a pathogenic paradox. Cell Metab. *7*, 95–96. https://doi.org/10.1016/j.cmet.2007.12.009.
12. Shimomura, I., Matsuda, M., Hammer, R.E., Bashmakov, Y., Brown, M.S., and Goldstein, J.L. (2000). Decreased IRS-2 and increased SREBP-1c lead to mixed insulin resistance and sensitivity in livers of lipodystrophic and ob/ob mice. Mol. Cell *6*, 77–86.
13. Li, S., Brown, M.S., and Goldstein, J.L. (2010). Bifurcation of insulin signaling pathway in rat liver: mTORC1 required for stimulation of lipogenesis, but not inhibition of gluconeogenesis. Proc. Natl. Acad. Sci. USA *107*, 3441–3446. https://doi.org/10.1073/pnas.0914798107.
14. Sun, F., Liao, Y., Qu, X., Xiao, X., Hou, S., Chen, Z., Huang, H., Li, P., and Fu, S. (2020). Hepatic DNAJB9 Drives Anabolic Biasing to Reduce Steatosis and Obesity. Cell Rep. *30*, 1835–1847.e9. https://doi.org/10.1016/j.celrep.2020.01.043.
15. Pajvani, U.B., Qiang, L., Kangsamaksin, T., Kitajewski, J., Ginsberg, H.N., and Accili, D. (2013). Inhibition of Notch uncouples Akt activation from hepatic lipid accumulation by decreasing mTorc1 stability. Nat. Med. *19*, 1054–1060. https://doi.org/10.1038/nm.3259.
16. Wu, X., Chen, K., and Williams, K.J. (2020). An oxide transport chain essential for balanced insulin action. Atherosclerosis *298*, 42–51. https://doi.org/10.1016/j.atherosclerosis.2020.02.006.
17. Kubota, N., Kubota, T., Kajiwara, E., Iwamura, T., Kumagai, H., Watanabe, T., Inoue, M., Takamoto, I., Sasako, T., Kumagai, K., et al. (2016). Differential hepatic distribution of insulin receptor substrates causes selective insulin resistance in diabetes and obesity. Nat. Commun. *7*, 12977. https://doi.org/10.1038/ncomms12977.
18. Vatner, D.F., Majumdar, S.K., Kumashiro, N., Petersen, M.C., Rahimi, Y., Gattu, A.K., Bears, M., Camporez, J.P.G., Cline, G.W., Jurczak, M.J., et al. (2015). Insulin-independent regulation of hepatic triglyceride synthesis by fatty acids. Proc. Natl. Acad. Sci. USA *112*, 1143–1148. https://doi.org/10.1073/pnas.1423952112.
19. Anderwald, C., Bernroider, E., Krssak, M., Stingl, H., Brehm, A., Bischof, M.G., Nowotny, P., Roden, M., and Waldhäusl, W. (2002). Effects of insulin treatment in type 2 diabetic patients on intracellular lipid content in liver and skeletal muscle. Diabetes *51*, 3025–3032.
20. Nascimbeni, F., Aron-Wisnewsky, J., Pais, R., Tordjman, J., Poitou, C., Charlotte, F., Bedossa, P., Poynard, T., Clément, K., and

Ratziu, V.; LIDO study Group (2016). Statins, antidiabetic medications and liver histology in patients with diabetes with non-alcoholic fatty liver disease. BMJ Open Gastroenterol. *3*, e000075. https://doi.org/10.1136/bmjgast-2015-000075.

21. Juurinen, L., Tiikkainen, M., Häkkinen, A.M., Hakkarainen, A., and Yki-Järvinen, H. (2007). Effects of insulin therapy on liver fat content and hepatic insulin sensitivity in patients with type 2 diabetes. Am. J. Physiol. Endocrinol. Metab. *292*, E829–E835. https://doi.org/10.1152/ajpendo.00133.2006.
22. Cusi, K., Sanyal, A.J., Zhang, S., Hoogwerf, B.J., Chang, A.M., Jacober, S.J., Bue-Valleskey, J.M., Higdon, A.N., Bastyr, E.J., 3rd, Haupt, A., and Hartman, M.L. (2016). Different effects of basal insulin peglispro and insulin glargine on liver enzymes and liver fat content in patients with type 1 and type 2 diabetes. Diabetes Obes. Metab. *18*, 50–58. https://doi.org/10.1111/dom.12751.
23. Gastaldelli, A., Stefan, N., and Häring, H.U. (2021). Liver-targeting drugs and their effect on blood glucose and hepatic lipids. Diabetologia *64*, 1461–1479. https://doi.org/10.1007/s00125-021-05442-2.
24. Petersen, M.C., and Shulman, G.I. (2018). Mechanisms of Insulin Action and Insulin Resistance. Physiol. Rev. *98*, 2133–2223. https://doi.org/10.1152/physrev.00063.2017.
25. Salinas, M., López-Valdaliso, R., Martín, D., Alvarez, A., and Cuadrado, A. (2000). Inhibition of PKB/Akt1 by C2-ceramide involves activation of ceramide-activated protein phosphatase in PC12 cells. Mol. Cell. Neurosci. *15*, 156–169. https://doi.org/10.1006/mcne.1999.0813.
26. Stratford, S., Hoehn, K.L., Liu, F., and Summers, S.A. (2004). Regulation of insulin action by ceramide: dual mechanisms linking ceramide accumulation to the inhibition of Akt/protein kinase B. J. Biol. Chem. *279*, 36608–36615. https://doi.org/10.1074/jbc.M406499200.
27. Powell, D.J., Hajduch, E., Kular, G., and Hundal, H.S. (2003). Ceramide disables 3-phosphoinositide binding to the pleckstrin homology domain of protein kinase B (PKB)/Akt by a PKCzeta-dependent mechanism. Molecular and cellular biology *23*, 7794–7808. https://doi.org/10.1128/MCB.23.21.7794-7808.2003.
28. Petersen, M.C., Madiraju, A.K., Gassaway, B.M., Marcel, M., Nasiri, A.R., Butrico, G., Marcucci, M.J., Zhang, D., Abulizi, A., Zhang, X.M., et al. (2016). Insulin receptor Thr1160 phosphorylation mediates lipid-induced hepatic insulin resistance. J. Clin. Invest. *126*, 4361–4371. https://doi.org/10.1172/JCI86013.
29. Lyu, K., Zhang, Y., Zhang, D., Kahn, M., Ter Horst, K.W., Rodrigues, M.R.S., Gaspar, R.C., Hirabara, S.M., Luukkonen, P.K., Lee, S., et al. (2020). A Membrane-Bound Diacylglycerol Species Induces PKC-Mediated Hepatic Insulin Resistance. Cell Metab. *32*, 654–664.e5. https://doi.org/10.1016/j.cmet.2020.08.001.
30. Samuel, V.T., Liu, Z.X., Wang, A., Beddow, S.A., Geisler, J.G., Kahn, M., Zhang, X.M., Monia, B.P., Bhanot, S., and Shulman, G.I. (2007). Inhibition of protein kinase Cepsilon prevents hepatic insulin resistance in nonalcoholic fatty liver disease. J. Clin. Invest. *117*, 739–745. https://doi.org/10.1172/JCI30400.
31. Abdul-Wahed, A., Guilmeau, S., and Postic, C. (2017). Sweet Sixteenth for ChREBP: Established Roles and Future Goals. Cell Metab. *26*, 324–341. https://doi.org/10.1016/j.cmet.2017.07.004.
32. Kim, M.S., Krawczyk, S.A., Doridot, L., Fowler, A.J., Wang, J.X., Trauger, S.A., Noh, H.L., Kang, H.J., Meissen, J.K., Blatnik, M., et al. (2016). ChREBP regulates fructose-induced glucose production independently of insulin signaling. J. Clin. Invest. *126*, 4372–4386. https://doi.org/10.1172/JCI81993.
33. Turner, N., Kowalski, G.M., Leslie, S.J., Risis, S., Yang, C., Lee-Young, R.S., Babb, J.R., Meikle, P.J., Lancaster, G.I., Henstridge, D.C., et al. (2013). Distinct patterns of tissue-specific lipid accumulation during the induction of insulin resistance in mice by high-fat feeding. Diabetologia *56*, 1638–1648. https://doi.org/10.1007/s00125-013-2913-1.
34. Smith, G.I., Shankaran, M., Yoshino, M., Schweitzer, G.G., Chondronikola, M., Beals, J.W., Okunade, A.L., Patterson, B.W., Nyangau, E., Field, T., et al. (2020). Insulin resistance drives hepatic de novo lipogenesis in nonalcoholic fatty liver disease. J. Clin. Invest. *130*, 1453–1460. https://doi.org/10.1172/JCI134165.
35. Wiegman, C.H., Bandsma, R.H.J., Ouwens, M., van der Sluijs, F.H., Havinga, R., Boer, T., Reijngoud, D.J., Romijn, J.A., and Kuipers, F. (2003). Hepatic VLDL production in ob/ob mice is not stimulated by massive de novo lipogenesis but is less sensitive to the suppressive effects of insulin. Diabetes *52*, 1081–1089.
36. Howell, G., 3rd, Deng, X., Yellaturu, C., Park, E.A., Wilcox, H.G., Raghow, R., and Elam, M.B. (2009). N-3 polyunsaturated fatty acids suppress insulin-induced SREBP-1c transcription via reduced trans-activating capacity of LXRalpha. Biochim. Biophys. Acta *1791*, 1190–1196. https://doi.org/10.1016/j.bbalip.2009.08.008.
37. James, D.E., Stöckli, J., and Birnbaum, M.J. (2021). The aetiology and molecular landscape of insulin resistance. Nat. Rev. Mol. Cell Biol. *22*, 751–771. https://doi.org/10.1038/s41580-021-00390-6.
38. Horton, J.D., Goldstein, J.L., and Brown, M.S. (2002). SREBPs: activators of the complete program of cholesterol and fatty acid synthesis in the liver. J. Clin. Invest. *109*, 1125–1131. https://doi.org/10.1172/JCI15593.
39. Haas, J.T., Miao, J., Chanda, D., Wang, Y., Zhao, E., Haas, M.E., Hirschey, M., Vaitheesvaran, B., Farese, R.V., Jr., Kurland, I.J., et al. (2012). Hepatic insulin signaling is required for obesity-dependent expression of SREBP-1c mRNA but not for feeding-dependent expression. Cell Metab. *15*, 873–884. https://doi.org/10.1016/j.cmet.2012.05.002.
40. Titchenell, P.M., Quinn, W.J., Lu, M., Chu, Q., Lu, W., Li, C., Chen, H., Monks, B.R., Chen, J., Rabinowitz, J.D., and Birnbaum, M.J. (2016). Direct Hepatocyte Insulin Signaling Is Required for Lipogenesis but Is Dispensable for the Suppression of Glucose Production. Cell Metab. *23*, 1154–1166. https://doi.org/10.1016/j.cmet.2016.04.022.
41. Leavens, K.F., Easton, R.M., Shulman, G.I., Previs, S.F., and Birnbaum, M.J. (2009). Akt2 is required for hepatic lipid accumulation in models of insulin resistance. Cell Metab. *10*, 405–418. https://doi.org/10.1016/j.cmet.2009.10.004.
42. Solheim, M.H., Winnay, J.N., Batista, T.M., Molven, A., Njølstad, P.R., and Kahn, C.R. (2018). Mice Carrying a Dominant-Negative Human PI3K Mutation Are Protected From Obesity and Hepatic Steatosis but Not Diabetes. Diabetes *67*, 1297–1309. https://doi.org/10.2337/db17-1509.
43. Michael, M.D., Kulkarni, R.N., Postic, C., Previs, S.F., Shulman, G.I., Magnuson, M.A., and Kahn, C.R. (2000). Loss of insulin signaling in hepatocytes leads to severe insulin resistance and progressive hepatic dysfunction. Mol. Cell *6*, 87–97.
44. Kotani, K., Peroni, O.D., Minokoshi, Y., Boss, O., and Kahn, B.B. (2004). GLUT4 glucose transporter deficiency increases hepatic lipid production and peripheral lipid utilization. J. Clin. Invest. *114*, 1666–1675. https://doi.org/10.1172/JCI21341.
45. Kim, J.Y., Garcia-Carbonell, R., Yamachika, S., Zhao, P., Dhar, D., Loomba, R., Kaufman, R.J., Saltiel, A.R., and Karin, M. (2018). ER Stress Drives Lipogenesis and Steatohepatitis via Caspase-2 Activation of S1P. Cell *175*, 133–145.e15. https://doi.org/10.1016/j.cell.2018.08.020.
46. Kim, Y.R., Lee, E.J., Shin, K.O., Kim, M.H., Pewzner-Jung, Y., Lee, Y.M., Park, J.W., Futerman, A.H., and Park, W.J. (2019). Hepatic triglyceride accumulation via endoplasmic reticulum stress-induced SREBP-1 activation is regulated by ceramide synthases. Exp. Mol. Med. *51*, 1–16. https://doi.org/10.1038/s12276-019-0340-1.
47. Nozaki, Y., Petersen, M.C., Zhang, D., Vatner, D.F., Perry, R.J., Abulizi, A., Haedersdal, S., Zhang, X.M., Butrico, G.M., Samuel, V.T., et al. (2020). Metabolic control analysis of hepatic glycogen synthesis in vivo. Proc. Natl. Acad. Sci. USA *117*, 8166–8176. https://doi.org/10.1073/pnas.1921694117.
48. Dentin, R., Pégorier, J.P., Benhamed, F., Foufelle, F., Ferré, P., Fauveau, V., Magnuson, M.A., Girard, J., and Postic, C. (2004). Hepatic glucokinase is required for the synergistic action of ChREBP and SREBP-1c on glycolytic and lipogenic gene expression. J. Biol. Chem. *279*, 20314–20326. https://doi.org/10.1074/jbc.M312475200.
49. Magkos, F., Su, X., Bradley, D., Fabbrini, E., Conte, C., Eagon, J.C., Varela, J.E., Brunt, E.M., Patterson, B.W., and Klein, S. (2012). Intrahepatic diacylglycerol content is associated with hepatic insulin resistance in obese subjects. Gastroenterology *142*, 1444–1446.e2. https://doi.org/10.1053/j.gastro.2012.03.003.
50. Kumashiro, N., Erion, D.M., Zhang, D., Kahn, M., Beddow, S.A., Chu, X., Still, C.D., Gerhard, G.S., Han, X., Dziura, J., et al. (2011). Cellular mechanism of insulin resistance in nonalcoholic fatty liver disease. Proc. Natl. Acad. Sci. USA *108*, 16381–16385. https://doi.org/10.1073/pnas.1113359108.
51. Ter Horst, K.W., Gilijamse, P.W., Versteeg, R.I., Ackermans, M.T., Nederveen, A.J., la Fleur, S.E., Romijn, J.A., Nieuwdorp, M., Zhang, D., Samuel, V.T., et al. (2017). Hepatic Diacylglycerol-Associated Protein Kinase Cepsilon Translocation Links Hepatic Steatosis to Hepatic Insulin Resistance in Humans. Cell Rep. *19*, 1997–2004. https://doi.org/10.1016/j.celrep.2017.05.035.
52. Zhang, Z., TeSlaa, T., Xu, X., Zeng, X., Yang, L., Xing, G., Tesz, G.J., Clasquin, M.F., and Rabinowitz, J.D. (2021). Serine catabolism generates liver NADPH and supports hepatic lipogenesis. Nat. Metab. *3*, 1608–1620. https://doi.org/10.1038/s42255-021-00487-4.
53. Polley, K.R., Miller, M.K., Johnson, M., Vaughan, R., Paton, C.M., and Cooper, J.A.

(2018). Metabolic responses to high-fat diets rich in MUFA v. PUFA. Br. J. Nutr. *120*, 13–22. https://doi.org/10.1017/S0007114518001332.

54. Charles-Messance, H., Mitchelson, K.A.J., De Marco Castro, E., Sheedy, F.J., and Roche, H.M. (2020). Regulating metabolic inflammation by nutritional modulation. J. Allergy Clin. Immunol. *146*, 706–720. https://doi.org/10.1016/j.jaci.2020.08.013.
55. Lyu, K., Zhang, D., Song, J., Li, X., Perry, R.J., Samuel, V.T., and Shulman, G.I. (2021). Short-term overnutrition induces white adipose tissue insulin resistance through sn-1,2-diacylglycerol/PKCepsilon/insulin receptor Thr1160 phosphorylation. JCI insight *6*, e139946. https://doi.org/10.1172/jci.insight.139946.
56. Flannery, C., Dufour, S., Rabøl, R., Shulman, G.I., and Petersen, K.F. (2012). Skeletal muscle insulin resistance promotes increased hepatic de novo lipogenesis, hyperlipidemia, and hepatic steatosis in the elderly. Diabetes *61*, 2711–2717. https://doi.org/10.2337/db12-0206.
57. Rabol, R., Petersen, K.F., Dufour, S., Flannery, C., and Shulman, G.I. (2011). Reversal of muscle insulin resistance with exercise reduces postprandial hepatic de novo lipogenesis in insulin resistant individuals. Proc. Nat. Acad. Sci. USA *108*, 13705–13709. https://doi.org/10.1073/pnas.1110105108.
58. Camporez, J.P., Lyu, K., Goldberg, E.L., Zhang, D., Cline, G.W., Jurczak, M.J., Dixit, V.D., Petersen, K.F., and Shulman, G.I. (2019). Anti-inflammatory effects of oestrogen mediate the sexual dimorphic response to lipid-induced insulin resistance. J. Physiol. *597*, 3885–3903. https://doi.org/10.1113/JP277270.
59. Diraison, F., Pachiaudi, C., and Beylot, M. (1996). In vivo measurement of plasma cholesterol and fatty acid synthesis with deuterated water: determination of the average number of deuterium atoms incorporated. Metabolism *45*, 817–821.
60. Lee, W.N., Bassilian, S., Ajie, H.O., Schoeller, D.A., Edmond, J., Bergner, E.A., and Byerley, L.O. (1994). In vivo measurement of fatty acids and cholesterol synthesis using D2O and mass isotopomer analysis. Am. J. Physiol. *266*, E699–E708.
61. Wadke, M., Brunengraber, H., Lowenstein, J.M., Dolhun, J.J., and Arsenault, G.P. (1973). Fatty acid synthesis by liver perfused with deuterated and tritiated water. Biochemistry *12*, 2619–2624.
62. Pfaffl, M.W. (2001). A new mathematical model for relative quantification in real-time RT-PCR. Nucleic Acids Res. *29*, e45.
63. Perry, R.J., Camporez, J.P.G., Kursawe, R., Titchenell, P.M., Zhang, D., Perry, C.J., Jurczak, M.J., Abudukadier, A., Han, M.S., Zhang, X.M., et al. (2015). Hepatic Acetyl CoA Links Adipose Tissue Inflammation to Hepatic Insulin Resistance and Type 2 Diabetes. Cell *160*, 745–758. https://doi.org/10.1016/j.cell.2015.01.012.
64. Samuel, V.T., Liu, Z.X., Qu, X., Elder, B.D., Bilz, S., Befroy, D., Romanelli, A.J., and Shulman, G.I. (2004). Mechanism of hepatic insulin resistance in non-alcoholic fatty liver disease. J. Biol. Chem. *279*, 32345–32353. https://doi.org/10.1074/jbc.M313478200.

STAR★METHODS

KEY RESOURCES TABLE

REAGENT or RESOURCE	SOURCE	IDENTIFIER
Antibodies		
Insulin Receptor	Cell Signaling Technology	Cat# 3020S; RRID:AB_2249166
Phosphorylated Insulin Receptor (Y1162)	Cell Signaling Technology	Cat# 3918S; RRID: AB_10548764
Akt	Cell Signaling Technology	Cat# 2920S; RRID: AB_1147620
Phosphorylated Akt (S473)	Cell Signaling Technology	Cat# 9271S; RRID:AB_329825
GSK3β	Cell Signaling Technology	Cat# 9832S; RRID:AB_10839406
Phosphorylated GSK3β	Cell Signaling Technology	Cat# 9331S; RRID:AB_329830
PRAS40	Cell Signaling Technology	Cat# 2691S; RRID:AB_2225033
Phosphorylated PRAS40	Cell Signaling Technology	Cat# 2997S; RRID:AB_2258110
FASN	Cell Signaling Technology	Cat# 3180S; RRID:AB_2100796
ACC	Cell Signaling Technology	Cat# 3662S; RRID:AB_2219400
PKLR	Proteintech	Cat# 22456; RRID:AB_10918271
Glucokinase	Santa Cruz Biotechnology	Cat# sc-7908; RRID:AB_2107620
HSP90	BD Biosciences	Cat# 610419; RRID:AB_397799
SREBP (2A4)	Santa Cruz Biotechnology	Cat# sc-13551; RRID:AB_628282
Actin (AC-15)	Sigma-Aldrich	#A1978; RRID:AB_476692
Chemicals, peptides, and recombinant proteins		
Deuterium Oxide	Cambridge Isotope Laboratories	Cat# DLM-4
Methanolic Boron Trifluoride	Sigma-Aldrich	Cat# B1252-100
Protease Inhibitor: cOmplete MINI	Roche	Cat# 11836153001
Phosphatase Inhibitor: PhosSTOP	Roche	Cat# 04906837001
Caspase Inhibitor: Ac-DMQD-CHO	Cayman Chemical	Cat# 27103
Regular Human Insulin	Novo Nordisk	Cat# NDC 0169-1833-11
Somatostatin-14	Bachem	Cat# H-1490
Somatostatin-28	Bachem	Cat# H-4955
Aminoglucosidase	Millipore-Sigma	Cat# A7420
[^{13}C2]acetyl-CoA	Millipore-Sigma	Cat# 658650
U^{13}C glucose-6-phosphate	Cambridge Isotope Laboratories	Cat# CLM-8367
Critical commercial assays		
Triglyceride SL	Sekisui	Cat# 236-60
Cholesterol E	Fujifilm	Cat# 999-02601
iTaq Universal SYBR Green	Bio-Rad	Cat# 1725121
Quantitect RT	Qiagen	Cat# 205311
Glucose SL	Sekisui	Cat# 235-60
Wako NEFA Kit	Fujifilm	Cat#s: 999–34691, 995–34791, 991–34891, 993-35191
Aspartate Aminotransferase Colorimetric Activity Assay Kit	Cayman Chemical	Cat# 701640
Glucose-6-Phosphate Assay	Millipore-Sigma	Cat# MAK014
Experimental models: organisms/strains		
C57BL/6 Mice	Jackson Laboratory	Strain#: 000664
Insr^{T1150A} C57BL/6 Mice		

(*Continued on next page*)

Continued

REAGENT or RESOURCE	SOURCE	IDENTIFIER
Oligonucleotides		
36b4 ***F***: GAGGAATCAGATGAGGATATGGGA		
36b4 ***R***: AAGCAGGCTGACTTGGTTGC		
Srebf ***F***: CGCCCATGAGTCGAGTAAGC		
Srebf ***R***: CGTCCCAGACATAGCACCAA		
Fasn ***F***: GAGGTGGTGATAGCCGGTATGT		
Fasn ***R***: GACCGCTTAGGCAACCCAT		
GcK (MGH Primer Bank ID#: 31982798a1) ***F***: TGAGCCGGATGCAGAAGGA		
GcK (MGH Primer Bank ID#: 31982798a1) ***R***: GCAACATCTTTACACTGGCCT		
Software and algorithms		
GraphPad Prism Version 9	Graphpad	https://www.graphpad.com/scientific-software/prism/
ImageJ	NIH	https://imagej.nih.gov/ij/
Adobe Illustrator	Adobe	N/A
Other		
Envigo 2018S diet	Envigo	Cat# 2018S
High Fat Diet (Research Diets D12492)	Research Diets	Cat# D12492
Silica Gel TLC Plates	EMD-Millipore	Cat# 1.05721.0001

EXPERIMENTAL MODEL

Animal care

C57BL/6 mice (7–12 weeks old) were obtained from Jackson Laboratory, and $Insr^{T1150A}$ mice and WT C57BL/6 littermates were obtained from an established colony.[28] Mice were individually housed under controlled temperature and lighting (12-h light/dark cycle, lights on at 7:00 a.m.) with free access to water and food. Mice were maintained with regular chow (RC: Envigo 2018S- 24% protein/58% carbohydrate/18% fat calories). During high fat diet (HFD) studies, the mice were given a special diet (HFD: Research Diets D12492: 20% protein/20% carbohydrate/60% fat calories) for a prescribed length of time (2 days, 9 days, or 4 weeks). All studies were performed with age-matched male mice; initiation of diet was staggered to achieve this (mice were studied at 11–16 weeks of age). For the last two days of HFD studies, water was supplemented with 1% dextrose. Surgeries were performed under isoflurane anesthesia, and carprofen analgesia was provided in the postoperative period. Animals were euthanized either with intravenous pentobarbital, or under isoflurane anesthesia. Care was taken throughout the study to minimize suffering. All experimental procedures were approved by and conducted in accordance with the Institutional Animal Care and Use Committee guidelines of Yale University School of Medicine.

METHOD DETAILS

In vivo hepatic *de novo* lipogenesis

Mice were fed HFD for 2 days, 9 days, or 4 weeks. In the final two days of the experiment, total body water deuterium enrichment was increased by injection (via intraperitoneal and/or subcutaneous route) of 23.4 mL/kg 0.9% NaCl in 99% ^2H enriched water (Cambridge Isotope Laboratories). Drinking water was supplemented 6% ^2H_2O and 1% dextrose after the injection. Food was withdrawn and the drinking water formulation was switched to 6% ^2H_2O without dextrose at 7 a.m. of the day of sacrifice; tissues were taken under isoflurane anesthesia at 1 p.m.

Fasting-refeeding studies

For all fasting-refeeding studies, mice were fed HFD for 2 days, 9 days, or 4 weeks. Two days prior to sacrifice drinking water was supplemented with 1% dextrose. Food was withdrawn and dextrose-supplemented water was replaced with plain drinking water between 6 and 7 p.m. the night before the study. HFD and 1% dextrose supplemented water was restored at 7 a.m., and tissues were taken under isoflurane anesthesia at 11 a.m.

Tissue triglyceride extraction

Lipids were extracted from tissues in ice-cold 2:1 chloroform:methanol. Lipids were extracted with shaking at room temperature for 3–4 h, and phase separation was achieved with H_2SO_4. Triglyceride content was measured using the Sekisui Triglyceride-SL kit (Sekisui).

Measurement of triglyceride *de novo* lipogenesis

Triglyceride palmitate deuterium enrichment was determined by GC-MS and *de novo* hepatic palmitate synthesis was calculated from isotopic data as previously described.[7,59–61] *Fatty acid deuterium enrichment by GC-MS:* Tissue lipid (in chloroform) samples were spotted onto Silica gel 60 plates, and TLC was performed with a mobile phase of hexane:diethyl ether:acetic acid (80:20:1). Plates were developed with 0.005% primuline in acetone:water (80:20). Purified samples were collected while absorbed to Silica and eluted with diethyl ester. Triglyceride-fatty acids were analyzed by GC-MS (5975CI, Agilent Technologies, Santa Clara, CA, USA) as fatty acid methyl esters following derivatization with methanolic boron trifluoride. The plasma ^2H_2O pool was assessed by exchange of hydrogens from plasma to acetone in the presence of sodium hydroxide; acetone deuterium enrichment was analyzed by GC-MS. *Calculation of %DNL:* The fraction of the hepatic palmitate pool newly synthesized during the experiment (F) was calculated as $F = ME \div (N \times p)$, where molar enrichment (ME) equals $m1+(2\times m2)$, where m1 and m2 are the atom percent enrichments (APEs) of singly and doubly deuterium-labeled palmitate; N is the number of exchangeable hydrogen atoms in a palmitate molecule, and p is the plasma APE of deuterium in water. Using the assumption that VLDL export and fat oxidation during the short duration of hyperinsulinemic clamp was minimal, the %DNL calculated for the clamp experiment was reported normalized to total hepatic triglyceride content.

Immunoblotting

Tissue was homogenized in ice-cold homogenization buffer with protease and phosphatase inhibitors (cOmplete MINI + PhosSTOP (Roche) + Ac-DMQD-CHO (Cayman)). Proteins were resolved by SDS-PAGE using a 15 well 4–12% gradient gel or a 26 well 4–15% gradient gel and electroblotted onto polyvinylidene difluoride membranes using a semi-dry transfer cell. The membrane was then blocked with 3% bovine serum albumin or 5% nonfat dried milk, and incubated overnight with primary antibody. After washing, membranes were incubated with horseradish peroxidase-conjugated secondary antibody (Cell Signaling Technology) for 60 min. Detection was performed with enhanced chemiluminescence; densitometry analysis was carried out using ImageJ (NIH). When data from multiple blots had to be combined for the same experiment, control samples were run on each gel/membrane to normalize the signal intensity between the blots. A complete list of primary antibodies is included in the reagent or resource table. When data from multiple blots had to be combined for the same experiment, control samples were run on each gel/membrane to normalize the signal intensity between the blots.

Quantitative PCR

Total RNA was isolated from tissue using standard kits (Qiagen, Germantown MD, USA). The abundance of transcripts was assessed by real-time PCR on an Applied Biosystems 7500 Fast Real-Time PCR System (Applied Biosystems, Foster City CA, USA) with an SYBR Green detection system (Bio-Rad, Hercules CA, USA). The expression data for each gene of interest were against a housekeeping gene as a control, and relative expression was determined using amplification efficiencies.[62] Primer sequences are included in the reagent or resource table.

Hyperinsulinemic-hyperglycemic clamp studies

Mice were fed an HFD for 2 days, 9 days, or 4 weeks. On the day of the study, food was withdrawn and water was switched to plain (no dextrose) drinking water at 7 a.m. Pre-infusion of 0.9% NaCl in 99% ^2H_2O at 3.3 μL/min started at 11 a.m., to a total infusion volume of 24.3 mL/kg. A 90 min somatostatin-augmented hyperinsulinemic-hyperglycemic clamp was performed starting at 1 p.m. During the clamp, all infusates were deuterium-enriched to 6% ^2H_2O, all saline flushes used during the study were deuterium-enriched to 3% ^2H_2O. Insulin was infused at 3 mU/(kg-min) to achieve a stable hyperinsulinemic state, a 1:1 mixture of somatostatin-14 and somatostatin-28 (w/w) was infused at 4 μg/(kg-min) to suppress endogenous insulin secretion,[18] and 20–40% dextrose was infused to achieve hyperglycemia, targeting plasma glucose level of 160–200 mg/dL or 200–250 mg/dL. Blood samples were collected by tail massage every 10 min. Mice were anesthetized with pentobarbital, tissues were snap-frozen.

Modified insulin tolerance tests

Mice were fed regular chow or HFD for 2 days, 9 days, or 4 weeks. Mice were fasted for 16 h prior to the study. Dextrose was added to the insulin injection to prevent confounders associated with hypoglycemia. Insulin (0.5 mU/kg) and dextrose (0.5 g/kg) were given by intraperitoneal injection. Blood samples were collected by tail massage at 0, 9, and 18 min; tissues were collected under isoflurane anesthesia at 20 min. Basal control mice were treated identically to the mice that received insulin, except they were euthanized prior to the injection.

Plasma biochemical assays

Glucose concentrations were determined using a YSI (2700 select) or with a standard kit (Sekisui). Standard kits were also used to measure plasma fatty acids (Fujifilm), triglycerides (Sekisui), cholesterol (Fujifilm), and aspartate aminotransferase (Cayman). Insulin concentrations were determined by radioimmunoassay (EMD Millipore).

Short chain CoA, glycogen, and glucose-6-phosphate measurements

Hepatic short chain and medium chain CoAs were assessed by LC-MS/MS, and hepatic glycogen content was determined biochemically as previously described.[63,64] Hepatic short chain and medium chain CoAs were extracted from 50 to 100 mg liver as previously described. Analysis was performed by LC-MS/MS (Shimadzu UFLCXR, Sciex 6500 QTRAP) by negative electrospray ionization. Parent-daughter ion pairs were monitored and quantified using internal standards ([$^{13}C_2$]acetyl-CoA).

For hepatic glycogen measurements, liver tissue was homogenized in 0.6 N perchloric acid, an aliquot was taken to proceed with glycogen hydrolysis, and a separate aliquot was taken to assess tissue free glucose. The sample taken for glycogen hydrolysis was neutralized with potassium bicarbonate, and incubated with aminoglucosidase (Sigma) at 40°C for 2–4 h.

Glucose-6-phosphate concentrations in overnight fed short term fasted mouse liver were measured with a commercially available kit (Sigma). After tissue homogenization, samples were deproteinized using a 10 kDa centrifugal filter, and glucose-6-phosphate concentrations were determined following the manufacturer's instructions.

Glucose-6-phosphate concentrations in hyperinsulinemic-hyperglycemic clamped mice were measured by tandem LC-MS/MS. Liver tissue was ground with a dry ice-cooled mortar and pestle. Extraction was performed with 0.5 mL of 50% methanol with a U^{13}C glucose-6-phosphate internal standard (50 μL of 400 μM). Centrifugal filtration was performed (0.22 micron filter followed by 100 kDa filter), and the filtrate was analyzed by a Sciex 6500 QTRAP LC-MS/MS adjacent with a Shimadzu prominence HPLC system and a Phenomenex Synergi Hydro-RP column. The method was set up with a Turbo Ion spray in negative mode with an MRM of 258.7/96.9 for glucose-6-phosphate and an MRM of 265.0/97.0 for the standard. The sample eluted out of the column with a two-solvent gradient: 15 mM Acetic Acid/10 mM tributylamine and Methanol.

QUANTIFICATION AND STATISTICAL ANALYSIS

Statistics

All data are the mean ± SEM, and any additional statistical data can be found in the figure legends and figures. Statistical analysis of the data was performed using GraphPad Prism Version 9 (Graphpad, San Diego, CA). When three or more groups were compared a one or two-way ANOVA with Tukey corrections for multiple comparisons or Kruskal-Wallis test with Dunn's correction for multiple comparisons was used. When two groups were compared, the Student's unpaired two-sided *t*-test was used. *p* values less than 0.05 were considered significant. Data was only excluded in the setting of experimental failure, e.g., line failure in an infusion study, failure to regain weight after surgery. Less than 10% of animals were excluded.